J|A|C|S ARTICLES

Published on Web 12/20/2010

Pair Distribution Function Analysis and Solid State NMR Studies of Silicon Electrodes for Lithium Ion Batteries: Understanding the (De)lithiation Mechanisms

Baris Key,[†] Mathieu Morcrette,[‡] Jean-Marie Tarascon,[‡] and Clare P. Grey*[,†,§]

Department of Chemistry, SUNY at Stony Brook, Stony Brook, New York 11794-3400, United States, LRCS, CNRS-UMR6007 Université de Picardie Jules Verne, 33 Rue Saint Leu 80039, Amiens, France, and Chemistry Department, University of Cambridge, Lensfield Rd, Cambridge CB2 1EW, United Kingdom

Received September 8, 2010; E-mail: cpg27@cam.ac.uk

Abstract: Lithium ion batteries (LIBs) containing silicon negative electrodes have been the subject of much recent investigation, because of the extremely large gravimetric and volumetric capacities of silicon. The crystalline-to-amorphous phase transition that occurs on electrochemical Li insertion into crystalline Si, during the first discharge, hinders attempts to link the structure in these systems with electrochemical performance. We apply a combination of local structure probes, ex situ ^{7}Li nuclear magnetic resonance (NMR) studies, and pair distribution function (PDF) analysis of X-ray data to investigate the changes in short-range order that occur during the initial charge and discharge cycles. The distinct electrochemical profiles observed subsequent to the first discharge have been shown to be associated with the formation of distinct amorphous lithiated silicide structures. For example, the first process seen on the second discharge is associated with the lithiation of the amorphous Si, forming small clusters. These clusters are broken in the second process to form isolated silicon anions. The (de)lithiation model helps explain the hysteresis and the steps in the electrochemical profile observed during the lithiation and delithiation of silicon.

1. Introduction

Rechargeable lithium ion batteries (LIBs) are currently the preferred energy storage devices in portable electronic devices, with the highest gravimetric and volumetric energy densities of all commercially available battery technologies.[1] Their potential use in hybrid and plug-in hybrid electric vehicles and all-electric vehicles (HEVs, PHEVs, and EVs) makes advances in this field more significant, because of both economic and environmental implications. Until the recent commercialization of Sony's NEXELION cells, the universally used negative electrode material in a LIB was carbon, because of its good capacity (372 mA h g^{-1} for graphite) and rate capability. However, there is still considerable interest in the development of high energy anodes. Silicon anodes are particularly attractive alternatives to carbon because of their extremely high gravimetric energy densities (3572 mA h g^{-1}). Compared to graphite, silicon also has a massive volumetric capacity of 8322 mA h cm^{-3} (calculated based on the original volume of silicon), which is again approximately 10 times that of graphite. Unlike carbon, the lithiation and delithiation mechanisms of Si are still unclear, because of the crystalline-to-amorphous phase transition that takes place during the first discharge of crystalline silicon,[2,3] the inability of conventional characterization methods such as diffraction hindering research efforts to study the structures of these largely amorphous systems.

The approximate composition of the lithiated amorphous silicon phase has been extracted from in situ X-ray diffraction studies, and ^{119}Sn Mossbauer studies of Sn-doped silicon have been used to probe the local structure around Sn and thus indirectly provide insight into the silicon local structures.[2,4−6] In our previous in and ex situ nuclear magnetic resonance (NMR) study, we acquired spectra from both the crystalline lithium phases within the lithium−silicon phase diagram and from the amorphous lithiated phases.[7]

We demonstrated that the ^{7}Li NMR shifts found for the crystalline lithium silicide phases ($Li_{12}Si_7$, Li_7Si_3, $Li_{13}Si_4$, $Li_{15}Si_4$, and $Li_{21}Si_5$) are correlated with specific local environments, lithium ions nearby silicide clusters, and isolated silicon anions giving rise to lithium resonances in distinct chemical shift ranges. $Li_{12}Si_7$ (containing $SiSi_3$ stars and Si_5 rings, Figure 1b) and Li_7Si_3 (Si−Si dumbbells/dimers, Figure 1c) give rise to ^{7}Li NMR resonances at approximately 18 ppm, while Li nearby the isolated Si ions found in $Li_{15}Si_4$ gives rise to signals at 6 to −10 ppm, the exact value depending on the state of lithiation of this phase (Figure 2).[7] The Li signal of $Li_{13}Si_4$, which contains both Si dumbbells and isolated ions, is at 12 ppm, an

[†] SUNY at Stony Brook.
[‡] Université de Picardie Jules Verne.
[§] University of Cambridge.

(1) Tarascon, J. M.; Armand, M. *Nature* **2001**, *414*, 359.
(2) Obrovac, M. N.; Christensen, L. *Electrochem. Solid-State Lett.* **2004**, *7*, A93.
(3) Obrovac, M. N.; Krause, L. J. *J. Electrochem. Soc.* **2007**, *154*, A103.
(4) Hatchard, T. D.; Dahn, J. R. *J. Electrochem. Soc.* **2004**, *151*, A838.
(5) Li, J.; Smith, A.; Sanderson, R. J.; Hatchard, T. D.; Dunlap, R. A.; Dahn, J. R. *J. Electrochem. Soc.* **2009**, *156*, A283.
(6) Danet, J.; Brousse, T.; Rasim, K.; Guyomard, D.; Moreau, P. *Phys. Chem. Chem. Phys.* **2010**, *12*, 220.
(7) Key, B.; Bhattacharyya, R.; Morcrette, M.; Seznec, V.; Tarascon, J. M.; Grey, C. P. *J. Am. Chem. Soc.* **2009**, *131*, 9239.

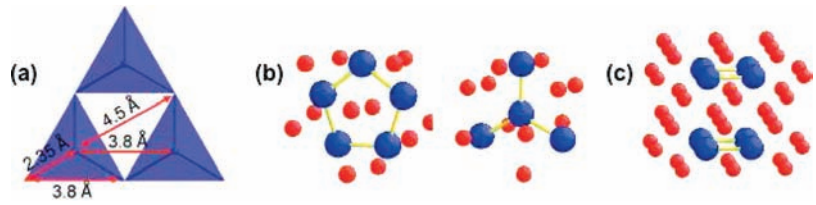

Figure 1. Local structures found in (a) crystalline silicon, (b) $Li_{12}Si_7$ (rings and $SiSi_3$ "stars"), and (c) Li_7Si_3 (dimers). The closest Si−Si contacts are marked with arrows in a. Blue and red balls represent Si and Li, respectively.

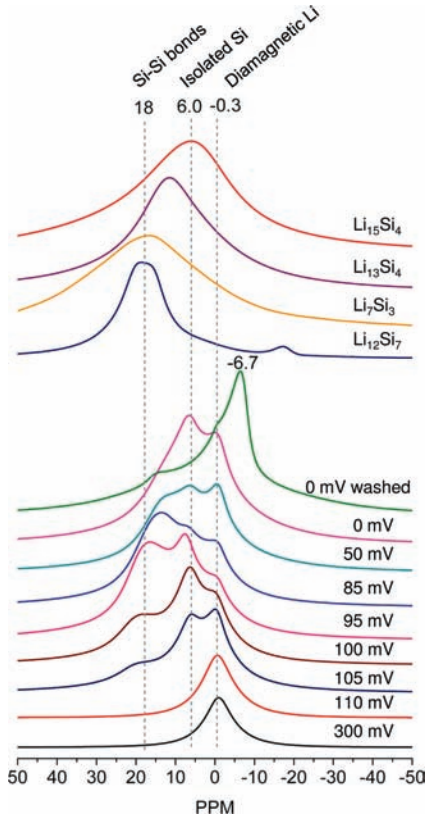

Figure 2. Ex situ ^{7}Li NMR of battery samples stopped during the 1st discharge of crystalline silicon. (Figure adapted from that shown in ref 7, with copyright permission from the American Chemical Society.) Two samples were prepared at 0 mV, the one entitled "0 mV washed" corresponding to a sample extracted very rapidly from a cell and washed, so as to limit the side reactions that are prevalent in this system, particularly for the fully lithiated phases.

intermediate between the two extremes. These shifts were then used to assign the lithium NMR resonances seen both in situ and from samples extracted from a battery at different states of charge (i.e., ex situ). This information was used to gain insight into the lithiation mechanism of crystalline silicon during the first discharge.[7] Our prior work also demonstrated that side reactions involving the lithiated silicides were significant, particularly for the fully lithiated phase $Li_{15+\delta}Si_4$. These side reactions were identified in our in situ NMR experiments on a working Li−Si cell; we demonstrated that the fully lithiated phases could only be captured in the ex situ experiments if the cells were disassembled very rapidly and the samples washed to remove electrolyte. The binder, CMC (carboxymethylcellulose), was shown to slow down this decomposition reaction significantly.

In the current work we use a combination of ex situ ^{7}Li magic angle spinning (MAS) NMR spectroscopy and X-ray pair distribution function (PDF) analyses to study the first and second cycles and identify local structures that are correlated with specific electrochemical signatures. Joint MAS NMR and X-ray and neutron PDF analyses have recently been successfully used to investigate short-range order in lithium ion battery electrode materials.[7−12] The combination of the two techniques should allow for an in-depth analysis of lithiation and delithiation mechanisms. Although X-rays are less sensitive to light elements, because of the *Z* dependence of X-ray scattering lengths, the X-ray PDF method will be sensitive to correlations involving silicon. By using a second local structure probe, PDF, we aim to extract further details concerning the silicon environments to support our lithium NMR results, which provide information concerning the local structures centered around lithium. We then combine this information to construct a model of lithiation and delithiation of silicon in the first and subsequent discharge−charge cycles.

2. Experimental Section

i. Electrochemistry. A series of samples were prepared for ex situ analysis by using 2032 type coin cells and by following a standard assembly procedure: The positive electrode was crystalline silicon powder (325 mesh, Aldrich), mixed with super P carbon in 1:1 weight ratio, and the negative electrode was lithium metal (0.38 mm thickness). 1 M $LiPF_6$ in a 1:1 volumetric mixture of anhydrous ethylene carbonate (EC) and anhydrous dimethyl carbonate (DMC) was used as the electrolyte (Merck, Selectipur). A porous borosilicate glass fiber soaked with the electrolyte was used as the separator. The cells were assembled in an argon glovebox and cycled galvanostatically either between 3.0 and 0.0 V or between 3.0 and 85 mV potential limits at a C/100 current rate with an Arbin Instrument galvanostat/potentiostat at room temperature. After electrochemical cycling, the cells were disassembled in the glovebox where the active materials were extracted, dried, and packed into 1.8 mm diameter zirconia rotors for MAS NMR analysis and into 1 mm diameter polyimide capillaries sealed with epoxy resin for X-ray scattering experiments at the synchrotron. The NMR spectra of the samples were run a few days after extraction. One 0 mV sample, called "0 mV washed", was extracted quickly from a cell and washed with DMC to investigate the lithium environments prior to any significant degradation of the lithium silicides, because of reactions with the electrolyte (a self-charge reaction). The second 0 mV "non-washed" sample was treated in the same manner as all the other higher voltage samples, a few hours passing between the end of discharge and the extraction of the sample from the battery. The PDF experiments were conducted days to weeks after the

(8) Jiang, M.; Key, B.; Meng, Y. S.; Grey, C. P. *Chem. Mater.* **2009**, *21*, 2733.
(9) Yamakawa, N.; Jiang, M.; Key, B.; Grey, C. P. *J. Am. Chem. Soc.* **2009**, *131*, 10525.
(10) Breger, J.; Dupre, N.; Chupas, P. J.; Lee, P. L.; Proffen, T.; Parise, J. B.; Grey, C. P. *J. Am. Chem. Soc.* **2005**, *127*, 7529.
(11) Breger, J.; Meng, Y. S.; Hinuma, Y.; Kumar, S.; Kang, K.; Shao-Horn, Y.; Ceder, G.; Grey, C. P. *Chem. Mater.* **2006**, *18*, 4768.
(12) Grey, C. P.; Dupre, N. *Chem. Rev. (Washington, DC, U. S.)* **2004**, *104*, 4493.

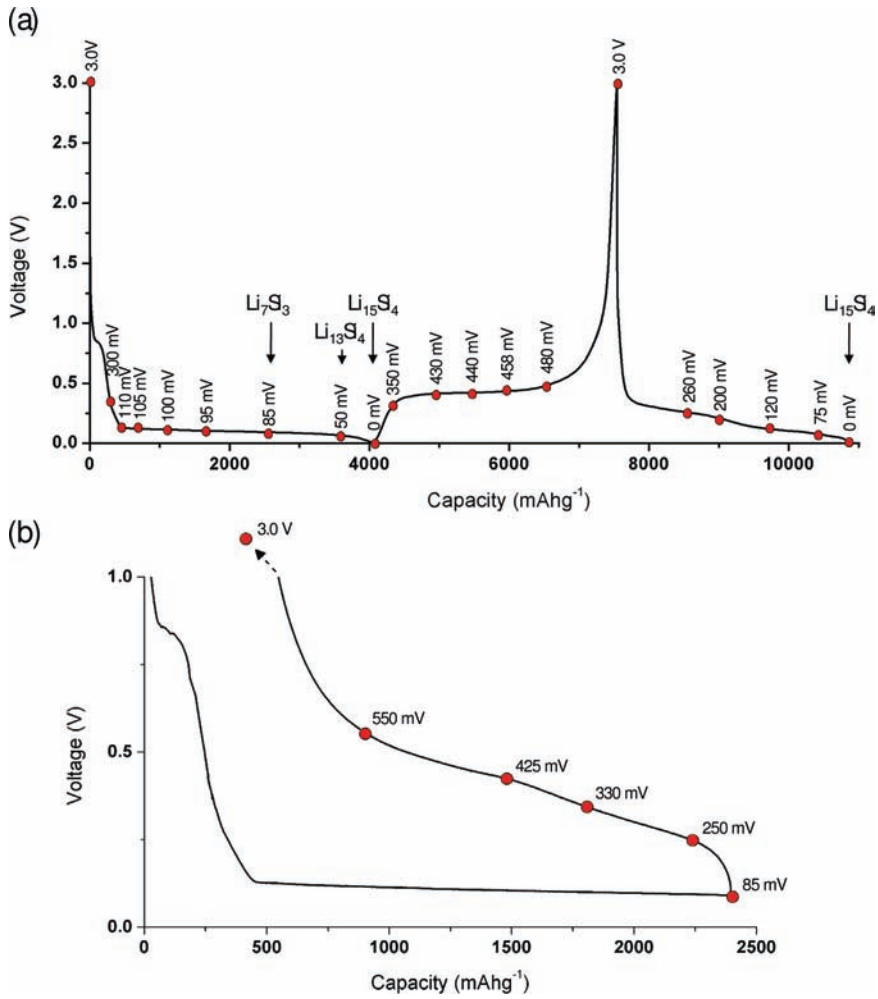

Figure 3. (a) The electrochemical profiles for the first discharge, first charge, and second discharge of crystalline silicon (voltage cutoffs between 3 and 0 V and with a C/100 current rate; approximate lithium silicide compositions of thermodynamic crystalline phases are marked with arrows). (b) The electrochemical charge profile following partial discharge to 85 mV. The last data point is collected at 3.0 V for b, but the *y*-axis is limited to 1 V so as to see the two distinct processes more clearly. The red points indicate the samples collected for ex situ PDF and NMR studies.

samples were extracted, so it is possible that some side reactions may have occurred.

ii. Diffraction and PDF. Total scattering patterns (Bragg diffraction patterns and diffuse scattering data) were acquired with two-dimensional (2D) detectors (GE a-Si and Perkin-Elmer a-Si 2D image plates) at the Advanced Photon Source in Argonne National Lab, IL (60 and 90 keV beam energies). 2D images were converted into 1D Q-space versus intensity plots by using the FIT2D program with a CeO_2 calibration standard, and PDF patterns ($G(r)$) were obtained with the PDFGetX2[13] software. The data range used was up to 23 A^{-1} Q. The PDFGui software[14] was used to fit the data. No attempt was made to subtract the PDF signal from the carbon.

iii. NMR. ^{7}Li MAS NMR spectra were acquired at 77.63 MHz using a CMX-200 MHz spectrometer, with a 1.8 mm MAS probe at a 38 kHz spinning speed. All of the ^{7}Li spectra were referenced to a 1 M LiCl solution at 0 ppm. Rotor-synchronized spin−echoes ($90° - \tau - 180° - \tau -$ acq) were used to acquire the spectra, where the values of τ were chosen, such that they were equal to the rotor period (i.e., $\tau = 1$/spinning frequency). A recycle delay of 0.2 s was used to collect a total of 32 000 scans for each sample.

3. Results and Discussion

Electrochemistry. An electrochemical profile that is typical of those from samples extracted from a series of different batteries is presented in Figure 3. The first (irreversible) process that occurs at approximately 0.8 V is primarily due to the reaction with the carbon in the Si/C composite and surface electrolyte interphase (SEI) formation. The lithiation of pristine crystalline silicon is accompanied by a long flat (slighting decaying) voltage region at approximately 125 mV. A nonstoichiometric $Li_{15+\delta}Si_4$ metastable phase has been shown to crystallize at the end of the first discharge, that is, on discharging to below 50 mV.[2,7,15] The subsequent charge (Figure 3a) is associated with a single, long plateau-like region at approximately 375 mV.[2] Galvanostatic intermittent titration technique, GITT, experiments (see Figure S2, Supporting Information (SI)) demonstrate that the processes on both discharge and charge are not true plateaus but are rather associated with gradual, sloping potentials. Two distinct processes are seen in the second discharge profile of silicon (Figure 3a), at approximately 250 and 100 mV, consistent with previous results[3] and GITT data (Figure S2, SI). The origin of these two

(13) Qiu, X.; Thompson, J. W.; Billinge, S. J. L. *J. Appl. Crystallogr.* **2004**, *37*, 678.
(14) Farrow, C. L.; Juhas, P.; Liu, J. W.; Bryndin, D.; Bozin, E. S.; Bloch, J.; Proffen, T.; Billinge, S. J. L. *J. Phys.: Condens. Matter* **2007**, *19*, 335219/1.
(15) Li, J.; Christensen, L.; Obrovac, M. N.; Hewitt, K. C.; Dahn, J. R. *J. Electrochem. Soc.* **2008**, *155*, A234.

processes is still not understood. Previous ^{119}Sn Mossbauer spectroscopy of Sn-doped amorphous Si electrodes also shows steps in the voltage composition curve and may provide indirect insight into the Si processes:[5] at a composition of $Li_{2.3}Si$ (at the end of the first process) the environment of the Sn becomes more symmetric, suggesting that each Sn (and thus *possibly* Si) atom is surrounded by only Li ions; that is, no clusters or Si−Sn directly bonded contacts remain.

Full lithiation during the second and any subsequent discharges to 0 V (Figure 3a) results in the crystallization of the nonstoichiometric $Li_{15+\delta}Si_4$ metastable phase and a charge profile that is similar to that seen on the first charge. A charge profile following a partial discharge to 85 mV (Figure 3b) results in two processes centered at 300 and 450 mV in the electrochemical profile, which can also be resolved in the GITT measurements (see Figure S3, SI) and whose origin again remains unclear. To throw some light onto these issues, two series of samples were investigated with NMR and PDF: the first to investigate the structural changes that occur following full discharge, and the second to explore the effect of partial discharge to 85 mV.

PDF and NMR Studies. First Discharge: PDF. The PDF studies of the crystalline lithium silicide phases clearly show distinct Si−Si and Li−Si atom−atom correlations and, thus, interatomic distances (see SI). Since the PDF data of these samples suggested that either some decomposition of the samples had occurred or (and) some phases contained significant concentrations of impurities and the quality of the data was poor for the highly lithiated phases, because of the low scattering power of Li, no detailed analysis of this data is included here. However, the data do show that the shortest Si−Si bond distance is seen for Li_7Si_3, the phase that contains Si−Si dimers with multiple bond character (2.38 Å for $Li_{12}Si_7$, 2.35 Å for Li_7Si_3). A more detailed direct analysis of Si−Si and Li−Si correlations was, however, attempted for the first discharge of crystalline silicon (Figure 4), and a more detailed discussion of the PDF of the model compounds is provided in the SI for comparison (Figure S1). While only the correlations to 9 Å are plotted in Figure 4, for the crystalline Si starting material, a series of correlations are observed that extend out to more than 40 Å. The first, second, and third peaks, at 2.35, 3.8, and 4.5 Å, correspond to the Si−Si bonds, the Si−Si contacts within the silicon tetrahedra (Si tet), and the Si−Si contacts between tetrahedra of the silicon diamond structure (Figure 1), respectively. As the discharge proceeds, the intensity of all Si−Si peaks decreases, but the correlations between more distant Si atoms decrease much faster than the correlations from directly bound Si and Si in the second coordination shell.

On discharging to 50 mV, all of the correlations at 4.5 Å have essentially disappeared, while the peaks at approximately 2.35 (Si−Si) and 3.8 Å (Si tet) still remain. The total loss of long-range order indicates that almost complete amorphization of crystalline silicon lattice occurs beyond 85 mV. The presence of the first two correlations, but the absence of the 4.5 Å peak, suggests that while some silicon tetrahedra or other smaller clusters remain, the long-range correlations between tetrahedra are destroyed. The 2.35 Å (Si−Si) correlation has shifted to 2.27 Å, indicating significant Si−Si multiple bond character and thus that a large contribution to this correlation now most likely originates from Si−Si dimers.

The appearance of a broad peak at 4.75 Å in both the "washed" and the "non-washed" 0 mV samples is due to the closest nonbonded Si−Si correlations, while the weak peak at

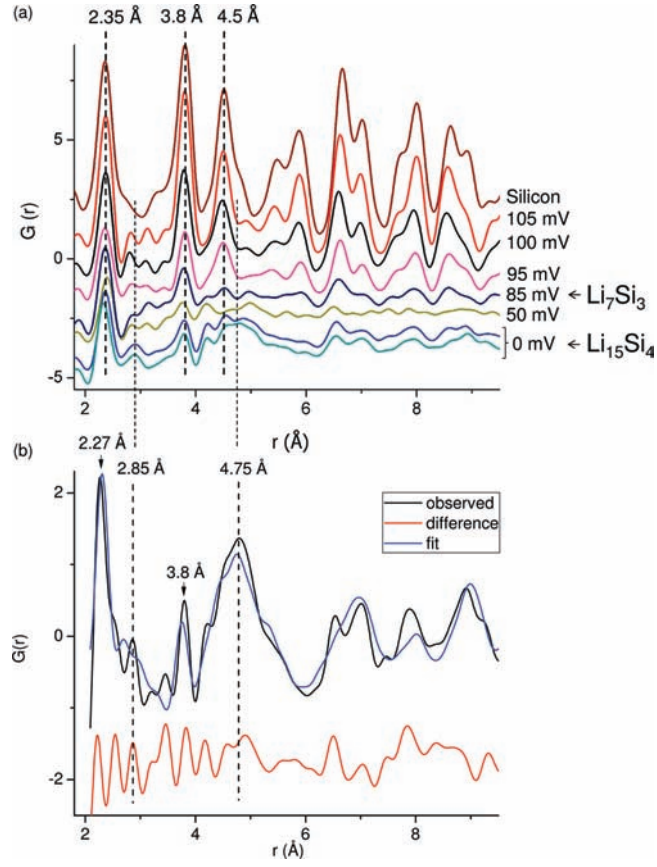

Figure 4. (a) Ex situ PDF of battery samples collected during the first discharge. The dashed lines correspond to the first, second, and third coordination shell Si−Si distances in a Si diamond matrix. Two 0 mV samples are included, the data shown in blue (top) representing the unwashed sample, while the data shown in teal (bottom) represents the washed sample. Approximate lithium silicide compositions are marked with arrows. (b) PDF data and fit (R_w = 43%) of the washed 0 mV sample. The dashed lines at 2.85 and 4.75 Å, connecting a and b, show characteristic $Li_{15}Si_4$ correlations.

2.85 Å is ascribed to Li−Si correlations, both being consistent with the formation of a $Li_{15+\delta}Si_4$-like phase at the end of the first long plateau-like region. Both samples produced similar PDF patterns indicating similar local structures. Clearly the relaxation process seen by NMR, due to the side reactions with the electrolyte, does not significantly affect the silicon correlations. Since differences between the relaxed and the nonrelaxed samples likely arise from disorder in the lithium sublattice, a future neutron PDF study may provide more insight into the structure of the lithium sublattice and any disorder. We note that both samples contain weak correlations that are close to those seen in crystalline Si. However, on the basis of the ^{29}Si NMR spectra of these samples reported in our previous study,[7] the concentration of residual Si is small.

The integrated areas under the 2.35, 3.8, and 4.5 Å peaks are plotted in Figure 5. Although the closest two Si−Si contacts still remain at the end of the discharge, the 3.8 Å Si−Si correlation, which corresponds to the edge of a Si tetrahedron (Figure 1a), is almost completely lost. These peaks are the weakest in the battery discharged to 50 mV, which may reflect more complete reaction of the Si in this particular battery, due to a better cell construction. In contrast, the batteries discharged to 0 V contain unreacted Si, in part due to poor cell construction. In addition, some decomposition of the $Li_{15}Si_4$ phase formed at this state of discharge, before the battery could be disassembled, or in the polyimide tubes used in the PDF experiments likely

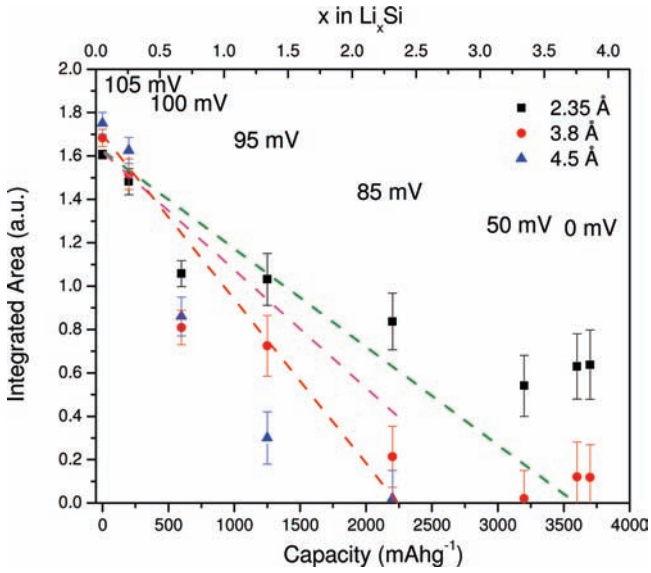

Figure 5. Integrated area under the peaks from the first and second Si−Si coordination shells, obtained from PDF of battery samples stopped during the first discharge at different indicated potentials. (For the two samples stopped at 0 mV (discharge capacity >3500 mA h g^{-1}), the points on the left and right correspond to the unwashed and washed electrode, respectively.) The green dashed line indicates the intensity loss predicted for both the 2.35 and 3.8 Å peaks, assuming a two-phase reaction from crystalline silicon to the $Li_{15+\delta}Si_4$ phase, while the magenta and red dashed lines correspond to the intensity loss predicted for the same two correlations, respectively, for a two-phase reaction to form the Li_7Si_3 phase.

occurs, these side reactions may possibly reform some Si−Si species, a phenomenon that was noted in our earlier NMR work.[7] A fit to the PDF data of the 0 mV sample (washed), performed using the crystalline structure of $Li_{15}Si_4$, is acceptable (Figure 4b) for distances greater than 3.8 Å; it is clear, however, that the crystalline structure does not capture all of the local distortions in this phase, and the material appears to contain considerable disorder. To provide an acceptable fit at short distances, silicon has been introduced as a second phase, but with a very large damping factor of 5.32 Å. The factor, which is also called nanoparticle amplitude correction parameter, dampens the calculated PDF appropriately according to the refined average nanoparticle diameter. This factor indicates that there are silicon-like clusters, which are on average no greater than 5.2 Å in size. There is also a minor crystalline Si component, which can be seen in the difference plots at longer distances (e.g., the peak at 6.5 Å).

To provide further insight into the mechanism by which silicon reacts with lithium, the theoretical loss in the intensities of the first three PDF correlations, if Si were to react via the two reactions,

$$7Li + 3Si \rightarrow Li_7Si_3\ (Li_{2.33}Si) \qquad (i)$$

(i.e., to form the phase containing $[Si\text{---}Si]^{4.66-}$ dumbbells, as in Figure 1c) and

$$15Li + 4Si \rightarrow Li_{15}Si_4 \qquad (ii)$$

(green dashes) is plotted. The first reaction should, in principle, be complete at a theoretical capacity of 2340 mA h g^{-1}, at which point Si−Si 2.35 Å correlations (magenta dashes) should still be present with approximately one quarter of the intensity of the same correlation in pristine Si. No 3.8 Å Si−Si correlations (red dashes) should remain. Alternatively, the direct, two-phase reaction of Si to form $Li_{15}Si_4$ should lead to a monotonic, simultaneous decrease of all of the Si−Si correlations along the path of the green dashed line. Except perhaps in the initial stage between 110 and 105 mV, where no clear difference (within the signal-to-noise ratio) is observed in the rate of change in the intensity of the first three correlations, both proposed reaction mechanisms do not describe the experimental change in intensity of the Si correlations, on discharge. The PDF data of the 100 and 85 mV samples (i.e., prior to approximately 2500 mA h g^{-1}) indicate that Si lithiation proceeds via the formation of clusters rather than the formation of isolated Si ions *only*, since the longer-range, nonbonded correlations drop more rapidly than expected for reaction i. The decrease in intensity of the correlations is similar, or even larger, than predicted by a model wherein Si reacts directly to form Li_7Si_3 (reaction ii) until after 95 mV. Thereafter, the absolute numbers of both 2.35 and 3.8 Å correlations are larger than predicted by the "Li_7Si_3" model. The behavior after 95 mV suggests that either (a) side reactions occur, so that the reaction proceeds more slowly than indicated by the current measured via the electrochemical measurements, and/or (b) clusters that are larger than a simple dumbbell are also present. Larger clusters are likely to be responsible for weaker correlations at 3.8 and 4.2 Å. For example, the Si−Si distances in the four-membered $Si(Si)_3$ "stars" in the crystalline material $Li_{12}Si_7$ (Figure 1b) contain Si−Si nonbonded distances of 4.05−4.19 Å and thus may contribute to the intensity of the 4.2 Å correlations. Assuming that the side reactions are not significant, at least above 50 mV, then if our cluster hypothesis, b, holds true, at 85 mV (i.e., at approximately the Li_7Si_3 stoichiometry) these clusters must also be accompanied by silicon environments that are richer in Li (i.e., environments that contain more Li in their local coordination shell, as found for isolated Si ions) than present in the thermodynamic phase for this composition (Li_7Si_3). Since the Li rich regions or clusters are in a more reduced state, this either implies a degree of compositional inhomogeneity across the electrode or that the activation energy associated with Si−Si bond-breaking is not sufficiently large to allow the system to reach local equilibrium, so that nonequillibrium structures (clusters) can persist, even in close proximity to each other. Most likely, both are true for this system.

Comparison with NMR Results. The PDF results are now compared with the previous NMR results on the same samples: Two ^{7}Li NMR resonances were seen for the 105 mV sample at 18 and 6 ppm, suggesting the presence of Li nearby Si−Si clusters (18 ppm) and Li nearby isolated silicon clusters (6 ppm). Both of these resonances gain in intensity until 95 mV. If the system followed the thermodynamic pathway, that is, phases with small clusters were formed first, then no resonance at 6 ppm would be expected during this stage of the reaction. The PDF data of the 105 mV sample is in agreement with the NMR data at this point and suggests the formation of both clusters and isolated Si ions, since the first three correlations appear to decrease in intensity together. The subsequent PDF data of the 100 and 95 mV samples do, however, appear to suggest that Si lithiation is largely proceeding via the formation of clusters, since the longer-range correlations drop more rapidly than the shorter-range correlations. This is consistent with the change in Li NMR intensities seen between the 100, 95, and 85 mV spectra, where the Li cluster resonance is seen to grow more rapidly than the resonance due to isolated Si. Note also that the NMR spectra, since they detect Li ions, will provide differently weighted information than the PDF data: An isolated silicon

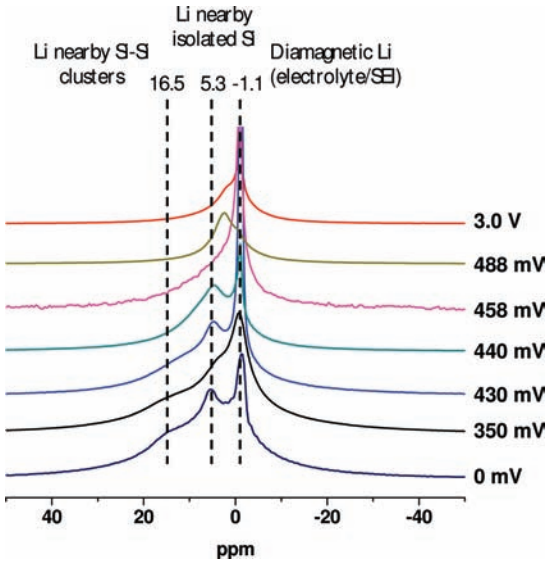

Figure 6. Ex situ ^{7}Li MAS NMR of battery samples stopped during the first charge. Dashed lines indicate resonances with known lithium assignments.

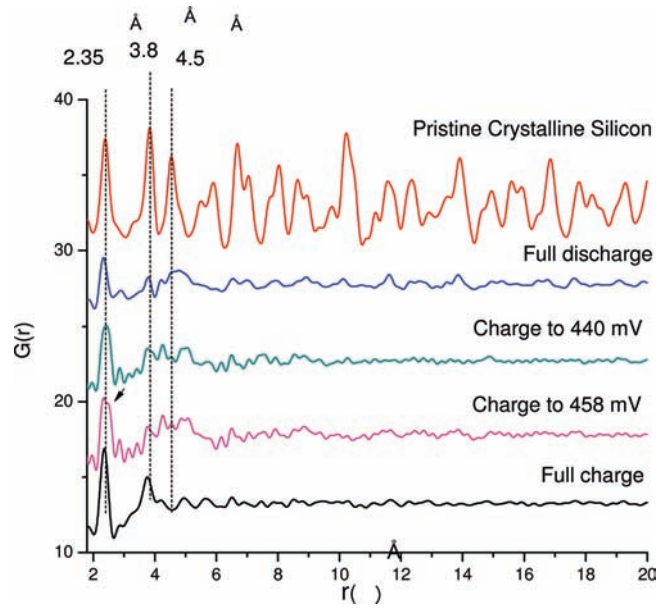

Figure 7. Short to mid-range ex situ PDF of crystalline silicon, fully discharged, charged to 440 and 458 mV, and fully charged battery samples extracted from the first cycle of a crystalline silicon electrode. The dashed lines indicate the first, second, and third coordination shells of Si in a Si diamond matrix. The arrow indicates the correlation at 2.5 Å.

anion will be surrounded by approximately 4 Li ions (3.75 in the $Li_{15}Si_4$ phase), while a silicon ion in the $Li_{12}Si_7$ or Li_7Si_3 phase will be nearby only 1.75−2.33 Li ions; more extended Si clusters will be nearby even fewer Li ions. Thus, the NMR data will overestimate the number of isolated Si anions. The slight shift and narrowing of the ^{7}Li "cluster" resonance between 100 and 95 mV, which coincides with a change in the rate of decrease in the intensities of the 2.35 and 3.8 Å correlations, suggests that different (likely smaller) clusters may be forming, and possibly that the Li mobility may be increasing (thereby resulting in narrower resonances). The significant concentration of Li nearby clusters in the 85−50 mV samples, as seen by NMR, is consistent with the PDF $G(r)$, where Si−Si bonds are still observed. The shift of the cluster resonance in this regime indicates that the Si−Si clusters are lithiated and broken, resulting in Li environments nearby both Si clusters and isolated ions (as found in the model compound $Li_{13}Si_4$) at 50 mV (resonance at approximately 13 ppm) and then predominantly nearby isolated Si clusters at 0 mV (6 ppm resonance). At the end of the first discharge, the ^{7}Li NMR spectra indicate that the sample is predominantly composed of Li nearby isolated silicon ions, again consistent with the PDF data. The weak higher frequency shoulder observed in the 0 mV sample indicates that residual Si−Si clusters are still present in the fully lithiated phase, consistent with the PDF results, where both Si clusters and residual crystalline Si were seen.

First Charge. The NMR spectra of samples collected along the pseudo plateau show a clear trend, a loss in the intensity of the NMR peaks seen as the charging proceeds (Figure 6). Up to a state of charge of 440 mV, which corresponds to the middle point on the charge, both the major resonance at 5.3 ppm due to Li in isolated Si clusters[7] and the minor resonance at 16.5 ppm due to Li in Si−Si clusters[7] lose intensity. Importantly, the spectrum of the sample from a battery stopped at 458 mV does not contain a resonance in the region between 16 and 18 ppm, where we expect the signal due to Li nearby small Si clusters (dumbbells or stars/rings) to appear, while the resonance at 5.3 ppm is still present. Thus, there is little evidence for the formation of intermediate phases or domains containing silicon clusters. Beyond this point to the top of the charge at 3.0 V, the resonance gradually shifts to 3−2 ppm. The 2 ppm resonance is tentatively ascribed to either some residual Li trapped in a lithiated silicide, in a "dead", that is, nonelectrically connected particle, or possibly some Li_2O due to the passivating layer of oxide on the surface of the starting material (the ^{7}Li chemical shift of Li_2O is 2.7 ppm[16]). An alternative explanation is that this resonance is due to Li particles nearby large silicon domains. More experiments are required to test this latter hypothesis.

The PDF data (Figure 7) are largely consistent with the NMR data: The 4.75 Å correlation due to long-range Si−Si ordering of isolated Si anions disappears by 440 mV (approximately the midpoint of the plateau-like region), the intensity of the first two Si correlations growing steadily with state of charge. The ratio of the intensities of these two correlations remains approximately constant with state of charge, this observation implying that no intermediates are seen: a higher intensity ratio for the 2.35:3.8 Å correlation, is characteristic of a cluster phase. A shoulder on the Si−Si peak is seen at 2.5 Å (marked with arrow for the sample collected at 458 mV). Interestingly, the crystalline LiSi phase, which contains a 3D three-coordinated Si network (analogous to black phosphorus) also contains longer Si−Si distances of 2.4−2.5 Å, suggesting that this correlation may be seen for similar Si local arrangements.[17] It is also possible that it is due to short Li−Si distances (see below).

The delithiated phase is amorphous and has only very weak peaks beyond 4 Å. The dominant peaks at 2.35 and 3.8 Å correspond to distances in a silicon tetrahedron. None of the smaller weaker peaks above 3.8 Å correspond to those found in crystalline Si, and the complete absence of the 4.5 Å peak indicates that the ordering between the Si tetrahedra that is present in crystalline silicon is completely absent. No nanocrystalline Si domains, which would be difficult to detect by diffraction, are formed. The difference in the 2.35:3.8 Å intensity

(16) Krawietz, T. R.; Murray, D. K.; Haw, J. F. *J. Phys. Chem. A* **1998**, *102*, 8779.
(17) Stearns, L. A.; Gryko, J.; Diefenbacher, J.; Ramachandran, G. K.; McMillan, P. F. *J. Solid State Chem.* **2003**, *173*, 251.

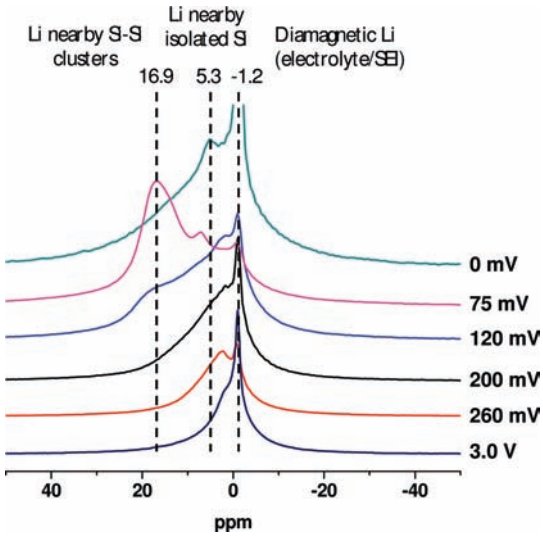

Figure 8. Ex situ ^{7}Li MAS NMR spectra of battery samples stopped during the second discharge. Dashed lines indicate resonances with known lithium assignments.

ratio between crystalline silicon and delithiated amorphous silicon indicates that the tetrahedra themselves are more distorted, and that some three-coordinate Si could also be present. The weaker peaks such as the one at 4.2 Å may correspond to Si−Si second coordination distances in three-coordinate Si units or in larger Si−Si rings, an increase in the Si−Si−Si bond angle leading to longer correlations.

Second Discharge. The lithiation of the amorphous Si, formed after the first charge, is now monitored by using both NMR and PDF, to investigate the structural origins of the two distinct voltage regions in the second discharge profile of silicon (Figure 3 and SI) at approximately 250 and 100 mV. Since subsequent discharge cycles appear to go through the same electrochemical processes[2], it is particularly important to understand these processes. Figure 8 shows the ^{7}Li NMR spectra of samples extracted following discharge after charging to 3.0 V. The first process, which starts at 300 mV and ends at approximately 150 mV, is accompanied by the appearance of a broad NMR resonance centered at around 3 ppm (see for example, the 260 mV sample). The NMR spectrum of the 200 mV sample is also dominated by the 3 ppm signal, but the presence of a tail at higher frequencies (centered around 12 ppm) indicates a minor presence of Li environments nearby Si clusters. The 3 ppm resonance is surprising, because on the basis of our earlier assignments it should indicate isolated Si ions. However, a 2−3 ppm resonance is also formed at the end of the first charge, where we suggested that it may be due to Li nearby much larger Si clusters. The observation of presumably the same resonance on both charge and discharge strongly suggests that this 3 ppm resonance is indeed due to Si nearby larger Si clusters, where little transfer of electron density between the Si clusters and the ionic Li^{+} ions has occurred; that is, the Li^{+} ions are still in a diamagnetic environment with a high partial charge. Again, this hypothesis requires testing.

Beyond 150 mV, the peak intensities change in a manner that is similar to that observed during the first discharge. After 200 mV, the resonance due to Li nearby small Si−Si clusters at 16.9 ppm starts to gain in intensity (along with the weaker resonance at approximately 8 ppm due to Li nearby clusters and isolated Si) until the end of the second plateau-like region at 70 mV. Beyond this point the 16.9 ppm resonance disappears,

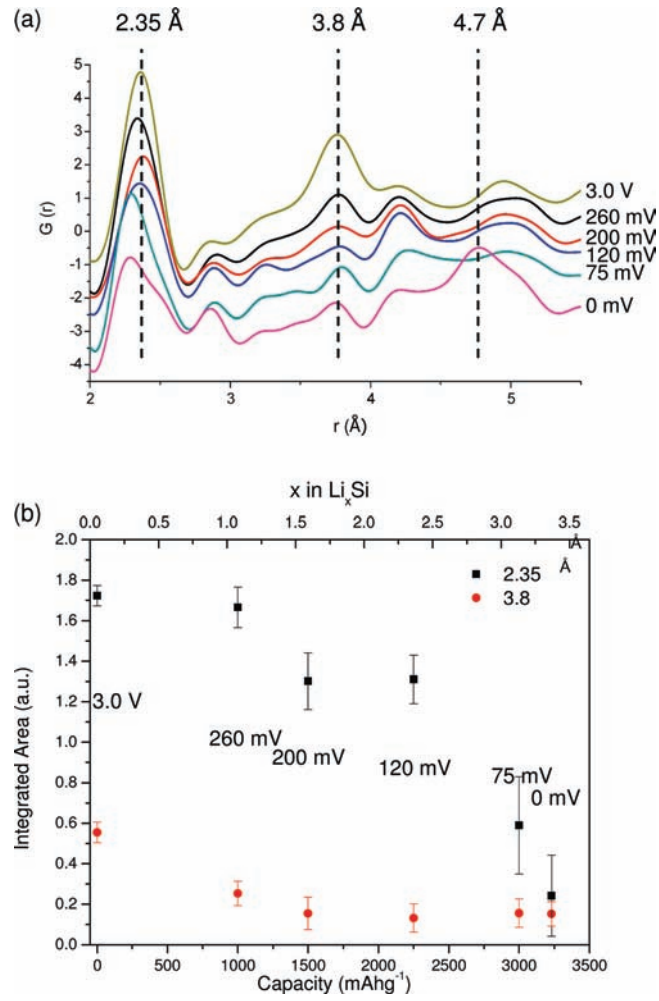

Figure 9. (a) Ex situ PDF $G(r)$ and (b) integrated area under the first two PDF correlations peaks, for battery samples stopped during the second discharge.

and at 0 mV, the 5 ppm resonance due to Li nearby isolated silicon ions dominates. The presence of an overlithiated $Li_{15+\delta}Si_4$ phase was detected in every subsequent discharge cycle after the first discharge[7] (see SI for an in situ NMR experiment that illustrates this (Figures S11 and S12)).

The short-range correlations in the PDF patterns (from 2−6 Å) and the integrated areas under the peaks for samples stopped during the second discharge are shown in Figure 9. The decrease in intensity of the 3.8 Å peak and the 2.35 Å peak does not follow the same trend as observed for the first discharge. The intensity of the 3.8 Å peak has diminished almost completely at the end of the first discharge plateau-like region, that is, in for the sample collected at 120 mV. However, the 2.35 Å peak is still present in the PDF pattern of this sample, indicating a complete loss of larger Si−Si−Si units, but the presence of residual Si−Si bonds in the structure. The peak at approximately 4.2 Å grows in this range, which we ascribe to the formation of Si "stars" (Figure 1b) or possibly Si−Si−Si trimers. Beyond this point, and along the lower voltage process at approximately 100 mV, the first coordination (Si−Si bond) peak continues to lose intensity. The PDF pattern of the 75 mV sample contains a new peak at approximately 2.5 Å, which is assigned to first shell Li−Si correlations. These correlations are clearly seen in the PDF patterns of the model compounds $Li_{12}Si_7$, Li_7Si_3, and $Li_{13}Si_4$ (see SI, Figure S1). At the same time, the "2.35 Å" peak

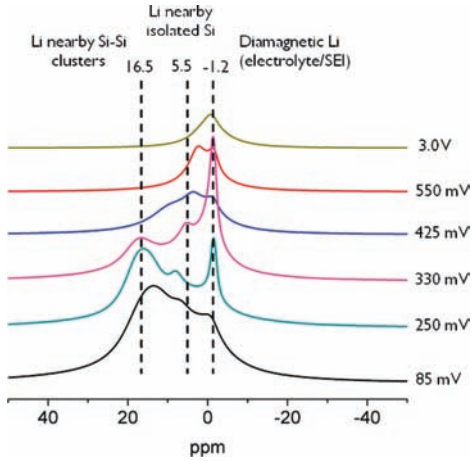

Figure 10. Ex situ ^{7}Li MAS NMR spectra of battery samples stopped during the first charge subsequent to a partial discharge to 85 mV.

shifts to lower values (approximately 2.30 Å), which we ascribe to the formation of more multiply bonded Si−Si linkages. The integrated "2.35 Å" peak intensity is strongly affected by the contribution from the 2.5 Å peak (Figure 9b), assigned to Li−Si correlations. Thus, the line shape was deconvoluted with two peaks (2.25 Å and 2.45 Å) for the 75 and 0 mV samples, and only the 2.25 Å deconvoluted integrated intensities are plotted. (see SI for this deconvolution and further discussion concerning the error bars). In summary, the plot of the Si−Si correlation intensities shows a decrease and almost complete loss of intensity of the 3.8 Å peak during the first higher voltage process, the 2.35 Å peak losing intensity during both processes, but most noticeably during the lower voltage process, some intensity remaining at the end of full discharge. At 0 mV, the characteristic distance at 4.7 Å due to the crystallization of the $Li_{15+\delta}Si_4$ can be observed.

Effect of Partial Discharging: First Charge. To investigate the correlation between structure and the two unexplained processes following a partial discharge,[2] a series of NMR spectra of samples were collected following discharge to a cutoff of 85 mV (Figure 3b) and subsequent charging. The cutoff voltage 85 mV is selected because it corresponds to a point near total amorphization of the crystalline silicon matrix. The studies described above indicate that, at this state of discharge, there are two main lithium local environments, lithium ions surrounding predominantly isolated Si ions (weaker resonance at approximately 8 ppm), and lithium ions close to Si−Si small clusters (14 ppm). Delithiation of this 85 mV phase to 250 mV is associated with a small shift of the 14 ppm (cluster) ^{7}Li resonance to higher frequency (16.5 ppm) and a loss of intensity of both the cluster and isolated Si, Li resonances (Figure 10). Both appear to suggest that larger clusters are formed at the expense of some of the isolated anions. The cluster resonance then decreases in intensity, and from 330 to 425 mV, it shifts to noticeably lower frequency, reaching 10 ppm at the end of the low voltage process. This change is ascribed to the noticeable and preferential delithiation of the Li nearby small Si−Si clusters. The 10 ppm resonance can be assigned to Li nearby both clusters and isolated Si based on the $Li_{13}Si_4$ resonance at 12 ppm, suggesting that the remaining Li does exist in these environments, presumably because the Li in environments nearby only clusters has already been removed. We note however that LiSi also resonates at 12.6 ppm,[17] and more experiments (utilizing ^{29}Si NMR) are in progress to establish the nature of some of the clusters more definitively. Beyond this point, the 10 ppm resonance completely disappears, and a shift of the 5.5 ppm resonance is observed, again to close to 3 ppm.

4. Discussion of the Lithiation Mechanisms

First Discharge. In general, lithiation is expected to start on or close to the surface of a Si particle, where the Li in electrolyte has access to the particle through the SEI. The significant volume expansion associated with lithiation of Si also favors a reaction front that starts from the surface. A recent density functional theoretical (DFT) study of lithium transport in crystalline silicon thin films found a large activation energy for lithium transport from the (100) surface into the bulk (0.88 eV), with lower activation energies for transport between subsurface sites (0.5 eV) and within the bulk (0.57 eV).[18] The larger activation energy largely resulted from the presence of a stable (low energy) site for Li on the silicon surface, these DFT studies again suggesting that the reaction starts by lithiating the surface. Presumably, the initial Li ions enter the Si framework from the surface sites forming interstitial sites. The presence of Li and the associated addition of electron density to the silicon framework will weaken the Si network surrounding Li, eventually resulting in Si−Si bond breakage and the formation of small Si (negatively charged) clusters surrounded by Li ions (Figure 11, II). Given (a) the large activation energy associated with Si−Si bond breakage, particularly for crystalline Si, and (b) the volume expansion associated with Li insertion, once Si−Si bond breakage has started, it will be (kinetically) easier to continue to break up these Si clusters, rather than to continue to lithiate and break up more of the Si framework. There will be a competition between the two processes (i.e., reaction with the framework, vs the clusters), both factors (i.e., the kinetics and the volume expansion) preventing the system from reaching thermodynamic equilibrium even if the potential is removed and the system is allowed to relax. Our results suggest that the intermediate phases such as Li_7Si_3 (containing dumbbells only) do not crystallize at this stage, because no single type of silicon cluster is present in the amorphous region. Crystallization to form one particular crystalline cluster phase would require Si−Si bond breakage and rearrangements (Si migration), which involves too large an activation barrier. The inhomogeneity of Li content likely occurs at both local and electrode level, the poor electronic conductivity of silicon likely contributing the latter inhomogeneity.

Such a scenario agrees with our PDF data, which shows a larger drop in intensity of the second and third Si−Si correlations over that expected in a reaction to directly form $Li_{15}Si_4$, indicating that clusters must be present. The 2.35 Å correlations are present throughout confirming that small clusters are present; their intensity at 85 mV (and the intensity of the 3.8 Å peak) is greater than predicted for a model where only dumbbells are present, showing that isolated Si ions must also be present, consistent with the NMR data at this stage. A comparison between the Li NMR data of Li_xSi and the model compounds again suggests that the Si clusters are relatively small, likely comprising dumbbells, stars, and possibly trimers/small rings.

The lithiation continues until all of the silicon atoms of the diamond matrix are consumed via bond breakage, as seen by PDF at beyond 85 mV (Figure 11, III, $Li_{2.33}Si$). At this point,

(18) Peng, B.; Cheng, F.; Tao, Z.; Chen, J. *J. Chem. Phys.* **2010**, *133*, 034701/1.

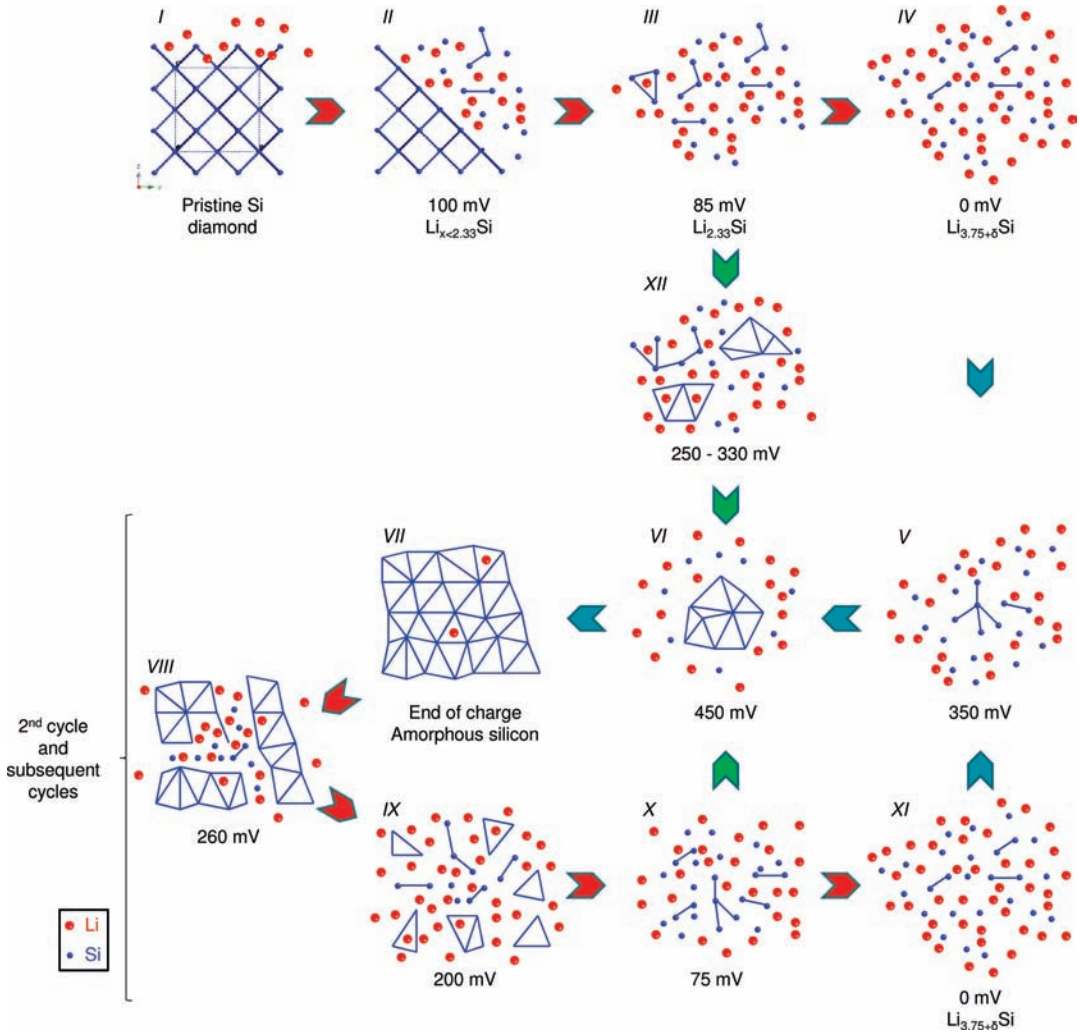

Figure 11. Illustration of mechanisms by which silicon is lithiated and delithiated. I to IV corresponds to lithiation of crystalline silicon discharged down to 0 mV. Red arrows denote discharge steps, while blue and green arrows denote charge steps. V to VIII correspond to the delithiation of fully lithiated silicon, and VIII to XI correspond to the relithiation of amorphous silicon to form fully lithiated silicon for cycle #x ($x > 1$).

a gradual shift of the NMR peaks to lower frequency, corresponding to the breakage of the small Si clusters, is seen, predominantly resulting in the formation of isolated silicon ions. A crystalline phase $Li_{15+\delta}Si_4$ can now (i.e., below 50 mV) nucleate from an amorphous $Li_{x'}Si$ phase, because the amorphous phase largely contains isolated Si anions and only a few Si clusters (Figure 11, IV). We speculate that one reason that the metastable $Li_{15}Si_4$ phase crystallizes rather than the thermodynamic phase $Li_{21}Si_5$ is because this phase can accommodate defects, such as Si−Si dumbbells, more readily than $Li_{21}Si_5$.

First Charge. The delithiation mechanism is shown in Figure 11 from IV to VIII. Contrary to the lithiation of crystalline silicon, delithiation from $Li_{15}Si_4$ may, in principle, proceed from both the surface and from the bulk owing to the high lithium diffusivity in the lithiated phases. Evidence for rapid Li motion in the Li_xSi phases comes from the sharp ^{7}Li NMR resonances that were observed in the static NMR spectra for the amorphous and crystalline lithiated phases[7] and for the lack of clear resolution of the signals from the different crystallographic sites in the ^{7}Li MAS NMR of the model compounds, even at spinning speeds of 38 kHz. Delithiation of $Li_{15}Si_4$ should lead to the formation Si clusters if delithiation follows the thermodynamic pathway, and yet these are not seen in significant concentrations in the Li NMR spectra (Figure 6). Thus, it appears that once a nucleation site, in the form of a small cluster is formed, this starts to grow to form an amorphous silicon matrix. Growth is helped by the rapid diffusion of Li^+ in the Li_xSi phase, away from the growing Si cluster/amorphous Si domain. Growth of an already formed cluster (or a defect that remains at the end of the first discharge) is more likely to dominate over nucleation to form a new cluster, because the latter requires two highly charged silicon anions (with formal charge of approximately 4−) in the $Li_{15}Si_4$ to migrate closer together and to combine. In contrast, addition of a Si anion to a growing Si nucleus (Si cluster) that has already formed, which will have a lower formal charge (per Si atom), should proceed more readily (Figure 11, V to VI). Thus, the lithiated phase with isolated Si ions is gradually converted to an amorphous Si phase. A few Li ions remain, as seen by the resonance at 3 ppm, but these are ascribed to Li on the surfaces of larger amorphous Si domains or coordinated to much larger Si clusters.

Second Discharge. The second discharge of the amorphous Si, based on the combined PDF and NMR studies, (Figure 11, from VIII to XI), progresses by breaking down the amorphous silicon matrix to form silicon clusters. The amorphous silicon matrix is more open than the crystalline one and thus can be more readily penetrated by lithium, resulting in almost complete

lithiation of the *whole* Si matrix by the end of the first (higher voltage) process. This is seen by the almost complete loss of the Si 3.8 Å correlation in the PDF experiment (Figure 11, IX) by 200 mV. The clusters that form at this point differ electronically from those of the model compounds: no resonances near 16 ppm are seen in the Li NMR experiment. They are also associated with an increase in intensity of the 4.2 Å PDF correlation. Beyond this point, the Si clusters are lithiated and further broken down (Figure 11, X) as seen by the decrease in the Si−Si 2.35 Å correlation and the appearance of the characteristic resonance at 16 ppm, due to Li nearby smaller Si clusters. At the end of the second full discharge, at 0 mV, the fully lithiated $Li_{15+\delta}Si_4$ phase recrystallizes (Figure 11, XI).

Charge Following a Partial Discharge. The different mechanism that follows partial discharge to 85 mV is ascribed to the presence of more Si clusters than at 0 mV. The residual clusters can serve as multiple nucleation sites within amorphous Li_xSi, these clusters growing during the lower voltage process, by the addition of isolated Si and presumably by fusing of some of the smaller clusters (Figure 11, green arrows, from III to XII to VII or from X to VI to VII) consistent with the change in the Li NMR spectrum from 85 to 250 mV. In the higher voltage process, the small clusters fuse to form larger amorphous Si domains as Li is extracted, and only a ^{7}Li signal near 3 ppm remains at 550 mV. Note that the Li spectra following the partial charge are very similar to that seen on lithiating the amorphous Si phase, the presence of the larger numbers of Si nuclei allowing delithiation to follow a pathway that is close to that seen on discharge.

5. Conclusions

A model for lithiation and delithiation of crystalline silicon is proposed on the basis of PDF and NMR results, to explain the electrochemical phenomena observed during the first discharge and all subsequent charge and discharge cycles regardless of the voltage cutoffs used for cycling. The model is composed of four mechanisms. Lithiation of crystalline silicon starts and progresses with bond breakage of the Si matrix from the surface by forming both lithiated isolated silicon anions and small lithiated silicon clusters until bulk crystalline Si is consumed and total amorphization is achieved. This is followed by breakage of the remaining Si clusters to form predominantly fully lithiated isolated silicon environments. The key to this mechanism is (i) the difficulty in breaking up the crystalline Si framework, which means that it is kinetically more favorable to lithiate silicon clusters and form isolated Si ions, or smaller clusters, than to break up the unreacted framework. (ii) Since a distribution of different Si clusters and anions are formed, the (more thermodynamically stable) crystalline phase expected based on Li:Si ratio of the amorphous component does not readily nucleate and grow, since this would involve Si−Si bond breakage and rearrangement of the clusters. Only when essentially all of the Si clusters are broken up (<50 mV) is it possible to nucleate a crystalline phase comprising isolated Si ions. The mechanism for delithiation of the fully lithiated phase progresses from a small number of nuclei, which are either formed on delithiation or which may still be present in the fully discharged phase. These nuclei grow directly to form the amorphous (delithiated) Si phase without (significant) formation of any intermediate structures or compositions with multiple small clusters. The amorphous Si phase formed on the top of charge contains Si tetrahedra, but no order beyond the silicon second coordination shell. On lithiation, the amorphous silicon matrix is much more open, so that the *whole* matrix can now be partially lithiated at the end of the higher voltage process (with a much lower overpotential than required to break the crystalline framework), partially breaking down the Si network. The lower electrochemical process is associated with the breaking down of the lithiated silicon clusters, and it ends with the recrystallization of the fully lithiated phase. If a partially delithiated phase, and one that still contains Si clusters, is delithiated, these clusters appear to serve nucleation sites, allowing the system to retrace a similar electrochemical pathway to that seen on discharge. In contrast, if the lithiation proceeds all the way to form $Li_{15}Si_4$, that is, the phase with isolated anions, there are few Si nucleation sites, and delithiation proceeds via the growth of only a few Si clusters which then grow to form larger Si domains and eventually the amorphous Si phase. Finally, we suggest that it it may be important to control the potential windows over which the material is cycled to optimize both the numbers and the type of clusters that are formed and that this may be important in determining the reversibility and capacity retention of this system. For example, cycling the material over the first process versus the second process involves very different rearrangements of the Si matrix or clusters, presumably with different kinetic barriers for reaction. Experiments are in progress to explore these suggestions.

Acknowledgment. This work was supported by the Assistant Secretary for Energy Efficiency and Renewable Energy, Office of FreedomCAR and Vehicle Technologies of the U.S. DOE under Contract No. DE-AC03-76SF00098, via subcontract No. 6517749 with the Lawrence Berkeley National Laboratory and via funding from the New York State Foundation for Science, Technology and Innovation NYSTAR award. This work has benefited from the use of the Advanced Photon Source at Argonne National Laboratory. We thank Peter Chupas, Karena Chapman, and Fulya Dogan for experimental support and Rangeet Bhattacharya and Chris Pickard for helpful discussions.

Supporting Information Available: PDF: PDF patterns of lithium silicon model compounds and samples extracted from batteries during the first charge of fully discharged electrodes; deconvolutions of the 2.35−2.5 Å correlation for the second discharge samples collected at 75 and 0 mV, supplied to illustrate the fitting procedure. Fits performed on PDF patterns of crystalline silicon, the $Li_{15}Si_4$ model compound, and fully discharged battery samples collected at the end of the first and second discharges. Electrochemistry: GITT plots of electrochemical experiments for the first three cycles of crystalline silicon versus Li/Li^+ with minimum potential cutoffs of 0 and 85 mV. NMR: stacked and contour plots of the in situ NMR experiment of crystalline silicon for the first three cycles. This material is available free of charge via the Internet at http://pubs.acs.org.

JA108085D